

System description and first light-curves of HAT, an autonomous observatory for variability search

G. Á. Bakos^{1,2}

*Harvard-Smithsonian Center for Astrophysics
60 Garden street, Cambridge, MA02138
gbakos@cfa.harvard.edu*

J. Lázár, I. Papp, P. Sári

*Hungarian Astronomical Association, H-1461 Budapest, P.O.Box 219
jlazar,ipapp, psari@mcse.hu
and*

E. M. Green

*Steward Observatory, University of Arizona, Tucson, AZ 85721
bgreen@as.arizona.edu*

ABSTRACT

Having been operational at Kitt Peak for more than a year, the prototype of the Hungarian Automated Telescope (HAT-1) has been used for all-sky variability search of the northern hemisphere. The small autonomous observatory is recording brightness of stars in the range of $I_c \approx 6 - 13^m$ with a telephoto lens and its $9^\circ \times 9^\circ$ field of view (FOV), yielding a data rate of $\sim 10^6$ photometric measurements per night. We give brief hardware and software description of the system, controlled by a single PC running RealTime Linux operating system (OS). We overview site-specific details, and quantify the astrometric and photometric capabilities of HAT. As a demonstration of system performance we give a sample of 60 short period variables in a single selected field, all bright, with $I < 13^m$, of which only 14 were known before. Depending on the observing strategy, search for extrasolar planet transits is also a feasible observing program. We conclude with a short discussion on future directions. Further information can be found at the HAT homepage: <http://www-cfa.harvard.edu/~gbakos/HAT/>.

Subject headings: instrumentation: miscellaneous – telescopes – techniques: photometric – stars: variables – methods: data analysis

1. Introduction

The idea of automating ground based observational astronomy goes back more than two decades. Minimizing manpower can assure uniform and massive data flow with low budget and

the absence of human mistakes.

The increasing number of robotic telescopes³ (capable of computer controlled multiple observations) have been used for a broad range of projects, such as astrometry: Carlsberg Meridian Telescope (Helmer & Morrison 1985); photoelectric photometry of pre-selected targets: Fairborn Observatory

¹Predoctoral Fellow, Smithsonian Astrophysical Observatory

²Konkoly Observatory, Budapest, H-1525, P.O. Box 67

³See eg. <http://alpha.uni-sw.gwdg.de/~hessman/MONET>

(Boyd et al. 1984); supernova search: KAIT (Richmond, Treffers, & Filippenko 1993); GRB follow-up: ROTSE (Akerlof et al. 2000; Smith et al. 2002) and LOTIS (Park et al. 1997, 2001), exoplanet searches: STARE (Brown & Charbonneau 1999), Vulcan (Borucki et al. 2001); and asteroid searches: TAOS (Chen 1999). The variety of targets is usually narrow, looking only for specific timescales, light-curve shapes and intensity ranges.

Although most projects concentrating on special targets gain a huge amount of photometric data, only few of them are capable of presenting their by-products to the astronomical community, e.g. OGLE (e.g. Woźniak 2002), MACHO (Allsman & Axelrod 2001) and ROTSE (Akerlof et al. 2000).

Initiated by ideas of Paczyński (1997), the All-Sky Automated Survey's (ASAS; Pojmański 1997) approach is different, in that the final goal has been photometric monitoring of *all bright stars* in a major part of the southern sky down to $I \approx 14^m$. Using a fully automated but inexpensive system consisting of an amateur-class CCD, a small telephoto lens and an equatorial mount, ASAS presented catalogues of 4000 bright variables from a 300° area of the southern sky, *96% being new discoveries* (Pojmański 1998, 2000). The upgraded ASAS-3 will produce an order of magnitude increase in the data flow.⁴ The incompleteness of our knowledge on bright variable stars was reinforced by Akerlof et al. (2000) who discovered 1781 new variables in a 2000° area.

Why is general variability study of bright objects important? Several answers can be found in Paczyński (1997, 2000), and others can be added. Variable stars are essential for testing stellar structure and evolution theories, examining galactic structure or establishing the extragalactic distance scale. Only bright variables are within the range of high resolution spectroscopy, parallax and proper motion measurements. Our knowledge of issues related to variable stars (e.g. distance scale) can be refined by the combination of detailed study of close-by, bright objects and of equidistant, homogeneous samples (e.g. OGLE – Galactic bulge, LMC, SMC). Serious incompleteness at the bright end affects all conclusions. A system-

atic, well-calibrated survey presents clean, statistically valuable samples with well defined limits for different subtypes of variable objects. A reliable database with sufficient and ever-growing timespan of light-curves can be used as an archive, for e.g., correlating optical variability with X-ray observations, made by satellites. It can be a valuable input to schedule big-telescope and space-mission observations, where telescope time is limited, or prior and longer-term data on field variables is necessary (e.g. the Kepler mission), furthermore, it can provide them with a real-time alert system of rare events. Such events can be nova explosions, helium flash of a star (Sakurai's object: Nakano & Kushida 1996; Duerbeck et al. 2000), super-outbursts of dwarf-novae (WZ Sge: Ishioka et al. 2001).

To mention specific examples, observational data is scarce for spotted red subgiant variables (RS Cvn, FK Com), which are crucial in understanding the stellar magnetic cycles. Detached eclipsing binaries (through their stellar mass, radius and luminosity determination) can be perfect distance and age indicators, if nearby systems are properly calibrated. Samples of such objects in the solar neighborhood are sparse (Paczyński 1997), partly due to their short and narrow eclipses, and lack of observational data (see Fig. 1 for our light-curve of a *semi-detached* binary). Bright contact binaries exhibit similar incompleteness, although long-term observations could reveal interesting phenomena, such as the transition to semi-detached state.

The Hipparcos Space Astrometry Mission presented us with discovery of a few thousand new bright variables, and the Hertzsprung-Russell (HR) diagram was described in terms of luminosity stability at the millimagnitude level (Perryman et al. 1997). However, Hipparcos observed only selected stars (120000 or $3/^\circ$), and the variable star sample is further limited by the ~ 110 epochs per star on average and cut-off at $I \approx 9^m$.

Mapping the location of the large variety of pulsating variables on the HR diagram is still far from being complete. Addressing phenomena, such as long-term period and amplitude modulations (e.g. Blazhko effect of RR Lyrae), evolution of the pulsational status of a star, is possible only by long-term and *homogeneous* observations. Given the huge data-flow, interesting phenomena

⁴http://www.astrouw.edu.pl/~gp/asas/asas_asas3.html

are expected to emerge, for instance further observational evidence for chaos in W Vir and RV Tau stars (Buchler, Serre & Kolláth 1995), triple-mode variables (GSC 40181807: Antipin 1997), Cepheids which stop pulsating (V19 in M33: Macri, Saselov, & Stanek 2001) or strong amplitude modulation of Cepheids (V473 Lyr: Burki et al. 1986). Long-term monitoring of semi-regular and Mira variables is needed to disentangle multiperiodicity and systematic amplitude variations (e.g. Kiss et al. 2000). The sample of the recently established γ Dor subtype (oscillations in non-radial gravity-mode) consists of only a few dozen stars. One example of the possibilities is our HAT-1 light-curve of the triple-mode pulsator AC And (Fig. 1).

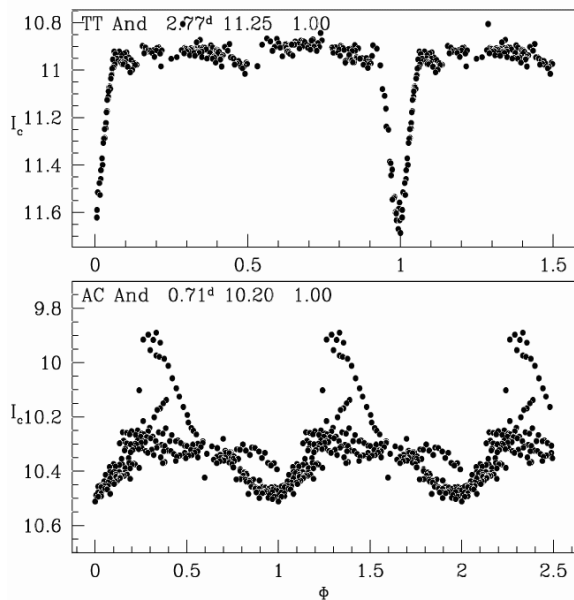


Fig. 1.— Phased light-curves of Algol-type, semi-detached eclipsing binary TT And, and triple-mode pulsator AC And from HAT observations (See §7). “Chaotic” appearance of the AC light-curve is due to its triple-mode behavior. Phase was computed from its longest period.

While the number of robotic telescopes is around a hundred, there are only a few completely autonomous observatories, where the human supervision is eliminated, and all auxiliary appliances (dome, weather station, etc.) are under a reliable computer control. These observatories can be installed to remote sites with adequate astro-

climate and infrastructure (electricity, Internet) without need of an on-site observer, and daily maintenance. The station can be monitored via Internet, and operation is not a bottleneck any more.

HAT is such a small autonomous observatory intended to carry out a northern counterpart of ASAS, i.e., a variability study of the northern sky. HAT was developed and constructed by one professional and three amateur astronomers⁵ in Hungary, and has been fully operational since May, 2001 at Steward Observatory, Kitt Peak, Arizona. HAT is controlled by a single Linux PC without human supervision.

The 180mm focal length and 65mm aperture of the telephoto lens, and the $2K \times 2K$ CCD yields a wide FOV: $9^\circ \times 9^\circ$ on the sky. Our typical exposure times allow us to study variability of the ~ 20000 objects per field brighter than $I_c \approx 13^m$ with few percent precision ($0.01^m - 0.05^m$), and few minute to one year time-resolution. As an extreme of the possible observing tactics, HAT is capable of recording the brightness of *every locally and seasonally* visible star in the range of $I_c \approx 6 - 13^m$ in every second day. Our limiting magnitude and photometric precision (See §7) corresponds to the following detection *cut-offs* for a few selected variability types (ranges indicate that the distance limit depends on the luminosity within the type): γ Doradus stars ($\langle 700pc$), δ Scuti ($1 - 2.5kpc$), RR Lyrae ($3kpc$), Cepheids ($10 - 150kpc$), Miras and semiregular variables ($\langle 60kpc$). The limits are based on the luminosity of the sources, and – especially at the larger values – overestimate true detection cut-offs, as they do not take into account reddening and crowding.

With the above specifications, HAT is also suitable for exo-planet search via transits, which is also included in our program. However, we concentrate on a broader range of variabilities: a large fraction of the sky is monitored sparsely, and few selected fields frequently so as to have preliminary results on short-period changes.

We expect that our survey will contribute to most of the aforementioned issues related to variability search (public archive, alert system), and

⁵G. Bakos (astronomical considerations and software), J. Lázár (software development; www.xperts.hu), I. Papp (electronic design) and P. Sári (mechanical engineering)

supplement the incomplete variable classes by new discoveries.

Our current data rate is roughly 10^6 photometric measurement, or two Gigabytes of raw data per night. Typically a few percent of the sources are variable, i.e., variable light-curves are supplemented by ~ 20000 data points each night.

HAT is monitoring only a fraction of the northern sky, but given the fact that it is an off-the-shelf system there is perspective for installation of new units in the near future.

The paper is arranged as follows: §2 gives an overview on the hardware, §3 describes our software environment, §4 quantifies the pointing precision of HAT, §5 and §6 summarize our site-specific installation at Kitt Peak and observations in the past one year, §7 estimates our photometric precision, §8 gives summary and future directions.

2. Hardware System

The HAT hardware consists of an equatorial telescope mount, enclosure (dome), CCD, a telephoto lens and a PC. Several devices are attached to the dome and telescope, such as rain-detector, photosensor, lens-heating and domeflat lights. The PC is protected from inclement weather by a close-by heated room (“warmroom”). Two parallel port cables with lightning protection connect the dome to the PC, and are responsible for driving the telescope and dome devices. Cables for the CCD depend on the specific setup; in our case a serial line for a Meade Pictor CCD (for testing purposes) and a custom data cable-pair for an Apogee AP10 CCD run from the PC to the telescope. A cable in a separate conduit carries 110V AC to the dome.

2.1. The Robotic Mount

Requirements of a mount for massive variability search are: reliability (for $10^5 - 10^6$ actuation), pointing to an accuracy of few orders of magnitude smaller than the FOV, ability to recover from awkward positions, never losing orientation, and relatively quick slew-time.

Our mount started as a replica of Gregorz Pojmański’s instrument for all-sky monitoring (Pojmański 1997), who kindly shared his plans with our group. The main mechanical concept of the mount is left unchanged, i.e., it is a backlash-free

friction drive of a horseshoe structure. Most of the details and dimensions, however, were re-designed. The mount is machined from forged aluminum alloy, to minimize the possibility of slow warpage, which could cause uncertainties in the pointing. All parts are anodized, to yield a tough and resistant surface.

The base of HAT is a $\sim 200\text{mm}\varnothing$ (diameter) disc, which can be mounted on a pier (see Fig. 2 for details of the mount). A rectangular steel plate can smoothly rotate on it, and can be fine-tuned by two adjusting screws, thus enabling the azimuth setting during polar axis adjustments.

The base frame of the telescope is held to the steel plate by a fixed screw and another screw freely running in altitude in a groove, for both sides. It can be gently adjusted in altitude $\pm 15^\circ$ (default center is 45°) with a spindle, much like the azimuth setting, and can be secured with the freely running screw. Inclinations outside these limits can be easily set by tilting the mounting of the base plate.

The horseshoe is supported at three points: the bearing-housing, a loose roller, and the right ascension friction-drive. The horseshoe outer diameter is $\sim 500\text{mm}$ with three arms attached to it in 120° spacings, forming a cone with pitch angle of $\sim 60^\circ$. The apex of this cone is the bearing housing of the RA axis with a high-precision ball-bearing inside. As the horseshoe is cut out from a larger piece of plate, relaxation of stress can change its shape, which affects tracking of astronomical objects. Thus, the whole structure is machined on a precision lathe as a piece later.

The horseshoe is constrained to the rollers by strong springs holding an arm and a small bearing running in the circular groove in the inner side of the horseshoe. The tight contact is crucial for proper positioning, as the not perfectly balanced horseshoe is friction driven, thus – especially at the extreme positions – torque is needed even for constant motion. The right ascension is driven by a five-phase stepper motor via sprockets and cogwheels and a stainless-steel roller with combined gear-ratio of 1 microstep of the motor = $1''$ (arc-sec) movement of the horseshoe. Slipping is further minimized by acceleration and deceleration of the mount in $\sim 50 - 100$ discrete velocity steps in an interval (“ramping”), both specified by the user at the software control. The steel wires of the

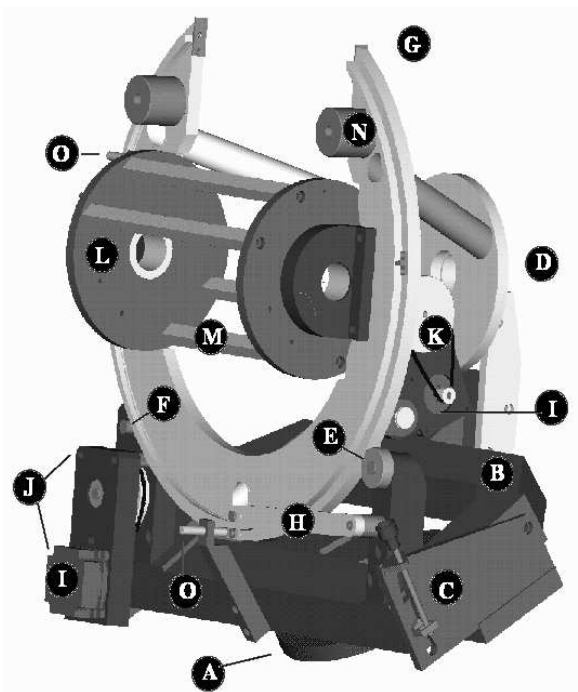


Fig. 2.— HAT mount drawing without the instrument mounting plate, CCD and lens. Labels on the image: A: main azimuth disc, B: rectangular base frame, C: altitude groove and adjusting spindle, D: RA bearing-housing and polar telescope hole, E: RA loose roller, F: RA friction-drive, G: horseshoe, H: horseshoe holding arm, I: RA and Dec stepper motors, J: RA driving mechanism: sprockets and cogwheels, K: Dec driving mechanism, L: Dec discs, M: Dec lateral bars, N: counterweights, O: proxy sensors.

sprockets prevent them from stretching, and yield a backlash-free drive. The maximal slew speed is $\sim 2^\circ/\text{sec}$.

The declination axis is made up of two $200\text{mm}\varnothing$ discs attached by bearings to the inner side of the horseshoe, and connected by four lateral bars, two of which hold the instrument-mounting plate. The axis is driven in a similar manner to the RA, i.e., by a 5-phase stepper, sprocket and cogwheels, but the final resolution is $5''/\text{microstep}$ and maximal speed is $\sim 5^\circ/\text{sec}$.

The maximal dimension of a telescope which fits our mount is $\sim 200\text{mm}\varnothing \times 400\text{mm}(l)$. The maximal size of the detector is limited by the inner half-sphere of the horseshoe, but most CCDs, such

as Apogee AP10 ($\sim 200 \times 200 \times 60\text{mm}$), fit readily. Balance of axes is achieved by counterweights on the top of the horseshoe, on the declination disc and on the instrument-mounting plate. The telescope (telephoto lens) is fixed to the instrument-mounting plate by a converter ring, and rigidly held by screws from the upper two lateral bars connecting the Dec discs, while the CCD is attached to the other side.

Inductive proximity sensors on both axes detect home and end positions in order to ensure fail-safe operation. Even though we use an open-loop control system (no costly encoder employed), and it might happen that the telescope loses orientation (due to e.g., power-failure), it can quickly recover by an iterative procedure of finding the home position. Physical end positions on both the RA and Dec axes guarantee that even if the proximity sensors fail, we cannot run off the rollers, and the telescope tube or detector never hits the mount.

Polar setting of the mount is simplified by the possibility of fitting a polar telescope to the central hole in the RA bearing house, and crude setting can be achieved in a few minutes. Final setting is done by standard methods such as described in Leung (1962) and references therein.

2.2. The dome

Automated, remote dome operations have to be perfectly fail-safe, because the detector can be damaged by inclement weather conditions, or the Sun might edge slowly across the field. A few of the encountered risks when closing the dome include gusty wind, power outage and failure of control software. In order to minimize software control and construction costs, and to enable rapid observation of targets of opportunity, only mechanisms that completely flip out of the way were considered. We designed a structure which proved to work in the past one year, with only a few minor failures. These failures, in turn, aided improvement of the design.

We experimented with simple schemes, such as a lid opening towards the north around the upper edge of the box, but this setup has strong wind resistance during the opening/closing phase. The standard rollover-roof structure is not compact enough and blocks a considerable part of the sky.

HAT mount is enclosed by a $\sim 0.6(w) \times 0.75(l) \times 0.75m(h)$ weather-proof box (See Fig. 3 for a schematic drawing). A separate slant roof on top is connected to the rest of the dome by swivel joints; a long bar is attached to its south corner and a shorter bar to the north, on both sides (assuming an installation on the northern hemisphere). The roof can be opened northwards by rotation around the bottom axes of the two arms, resembling an asymmetric clamshell. As the lengths of the arms differ, the roof co-rotates in such a way that resistance against wind is minimal in every position, and eventually it gets blocked from the wind behind the bulk of the dome, with its hollow part facing down. The longer bar has counterweights on the bottom such that the dome closes even if the driving mechanism is broken, simply through gravity.

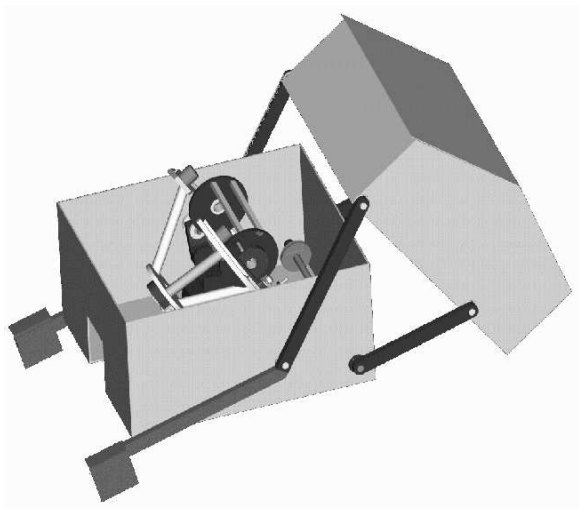


Fig. 3.— Half-open dome of HAT. The asymmetric clamshell structure ensures fail-safe operation and minimal resistance against wind.

The shorter bar is fixed to a shaft inside the dome, which is driven by a windshield-wiper DC motor through low gear ratio. Two sensors detect if the dome reached any of its end positions (closed or open). Safety power supply for the motor is a 12V 7.5Ah battery, continuously recharged from the main PC power supply of the dome, which in turn is connected to the UPS in the warmroom. Even without recharging, this battery would be able to open/close the dome several times a day for a week, though there is no need

for this, as power failures are detected by the software, and the system is automatically shut down. Although normally the PC controls dome operations, a light sensor on the bottom of the dome acts as a “big-brother”, and closes the dome if illuminance reaches that of a dawn/dusk sky. Similarly, a research grade Vaisala rain-detector has the capability of emergency closing.

Due to problems with skyflat frames (see later in §6) a domeflat screen is fixed to the inner north roof, and lit by small bulbs from positions which yield almost even illuminance not affected by the telescope’s position. When the telescope is pointed to the north pole, the screen is perpendicular to its aperture. Rotation of the entire mount about the pole averages out approx. half of the residual illuminance pattern.

Dome operations can be also performed manually, overriding other control. All electronics are installed in a separate compartment on the south wall, and can be easily dismantled from the outside for servicing without opening the dome.

2.3. Electronics

The electronic cards and devices in the dome are connected to the 12V DC outputs of a simple PC power supply, which in turn gets power from the warmroom’s UPS. Some devices are also connected to the re-chargeable battery, and can be operated even during power failure. One card is responsible for control of the mount, another for all other devices, including the dome.

Signals coming from the parallel port of the PC are optically isolated, and micro-controller units convert them for direct control of the stepper motors. Cards are simply *converters*, and the motordrive/clockdrive is the PC’s central processing unit, controlled by the RTLinux OS.

2.4. The CCD

HAT has been operated with two CCDs. The camera during the test period of 2000/2001 from Budapest, Konkoly Observatory, was an amateur-class **Meade Pictor 416xt** camera with a Kodak KAF-0401E chip of 512×768 , $9\mu m$ pixels. This camera yielded noisy images with bad electronic interference pattern and functioned erratically, but was suitable for test-mode operation (Pojmański 1997; Bakos 2001, for more details).

All astrometric calibration described in §4 was performed with this CCD.

The current Kitt Peak setup uses an **Apogee AP10** camera with Thomson THX 7899M 2K \times 2K, 14 μ m, grade 2 chip. The chip covers $\sim 29 \times 29$ mm, i.e., comparable to the size of small format photographic films (24 \times 36mm). Full-well capacity is 200,000 e^- , factory gain setting is 10 e^- /ADU, thus given the 14-bit (16000 ADU) dynamic range, saturation is slightly limited by the A/D conversion. Quantum efficiency of the Thomson chip peaks at 40% between 650nm – 800nm.

Readout noise is variable, being $\gtrsim 20e^-$. Bias level is 270 ± 5 ADU (nightly variation), with considerable long-term (day-to-day) instability of ± 15 ADU. Dark current at -15°C is ~ 0.05 ADU/sec and highly dependent on temperature setting (~ 0.02 ADU/sec at -25°C). We would like to keep the temperature of the system at a constant level throughout the year for the uniformity of the data. Unfortunately the two-stage Peltier cooling is capable of only $\Delta T \approx 30^\circ\text{C}$, and the lowest value we can achieve is -15°C .

The camera is connected to the PC by a data and a control cable plugged into an ISA-card. The cable length in our setup is 18m, much longer than the factory default (8m), although well below the company-claimed maximum limit. This caused problems during the installation, and hindered us from using the camera for the first 3 months, as the images contained only a few bits. Typical readout time of a frame is $\lesssim 10$ sec at 1.3MHz speed, so there is negligible dead-time due to readout.

Bias frames have a distinct, relatively constant pattern; few bad columns, many warm pixels, horizontal streaks and clusters of warm pixels. Dark frames have similar structure, which does not completely disappear after bias correction. About 10% of the frames have anomalous noise and background, the latter is $\sim 10 - 20$ times higher than the normal. Most likely these frames are due to a bug in the readout electronics.

2.5. The Telephoto Lens

In principle any kind of telephoto lens or small telescope can be attached to HAT's mounting plate, which has dimensions smaller than as described in §2.1. Our choice of a Nikon 180mm f/2.8 manual focus telephoto lens (64mm \varnothing) for the

Kitt Peak setup was motivated by several factors, such as our limited budget, the acceptable quality of Nikon lenses, and approximate compatibility with the ASAS-2 project, which uses 200mm focal length with the same Apogee CCD (Pojmański 2002).

The resulting FOV is $9^\circ \times 9^\circ$, where one pixel corresponds to $\sim 16''$. The lens gives moderately sharp profiles throughout the entire field, with half-width of the psf $\sim 1.6 - 2.0$ pixel (25'' – 32''). The corners show some coma and astigmatism. There is substantial field-dependent vignetting, reaching a 40% intensity loss near the edges, which is not surprising at lenses designed for small-format photography.

A strong resistive heating of the lens is installed in the light-baffle (dew cap). This not only prevents formation of dew on the front lens, but also creates turbulence to blur the stellar profiles to some extent. As our psf is undersampled, we have deliberately blurred the image in this way in an attempt to improve photometry (Pojmański 2002, and §7). Slight defocusing of the lens is not possible, as it introduces strong, spatially dependent distortion of the profiles.

We observe through a single Cousins I-band filter (Bessel-made), which has favorable combined sensitivity with the Thomson chip, yielding considerably higher signal-to-noise ratio for typical stars and integration times than e.g. a V filter would. The brightness of the night sky is more stable in I-band at different lunar phases (Walker 1987), $I \approx 19.9^m/\square''$ (new moon) to $I \approx 19.2^m/\square''$ (full-moon), as compared to e.g. $V \approx 21.8^m, 20.0^m$, which ensures more uniform photometry. New filters can be inserted only manually.

2.6. The PC

Any reasonable ($\gtrsim 300$ MHz) personal computer which can run a Linux Operating System and real-time kernels⁶, and has two parallel ports, is suitable for controlling the HAT mount and dome. An ISA-slot is requisite for controlling the Apogee AP10 CCD, and serial line is needed for the Meade Pictor CCD.

⁶As of writing, Real-Time Linux 3.1, kernels (core of the OS) 2.2.19 or 2.4.*.

We use a custom-built PC with 900MHz Athlon AMD processor, 256Mb RAM, DAT-DDS3 tape archiving facility, and a single 80Mb disc for temporary storage. Outgoing cables are lightning-protected. Power is from a UPS plugged in the same circuit as the UPS for the dome power supply. A watchdog-card automatically hard-resets the computer if that freezes (does not respond via a special software) for more than 10 minutes.

3. Software System

Our control PC runs an ordinary Linux OS with a Real-Time Linux kernel⁷(denoted RTLinux). Accurate positioning (e.g. sidereal speed tracking) needs precisely scheduled stepping instructions from the control electronics, with the possibility of frequency tuning (adjusting the tracking speed) and switching between speeds (e.g. ramping). These are either directly emitted by a complex external hardware with built-in frequency standard, *or by the computer* and its central processing unit (in fact a very complex hardware, but off-the-shelf). Both approaches have pros and cons, but we found the latter more flexible, because software can be adjusted remotely, and because it requires less hardware development. The CPU’s capability of emitting signals with a tight schedule depends on the OS. With “single task” operating systems, such as DOS, proper scheduling of a *single* task was possible. However, a further demand is that simultaneously with signal-generation, one should be able to execute other tasks, such as CCD operation, disc IO, etc., each of them requiring some CPU time, thus distorting the frequency of the high priority processes requesting periodic operations.

RTLinux is such a *real-time, multitask* operating system, where the kernel treats the real-time processes as independent “threads” with response times better than $15\mu s$. The Linux environment, the user’s interface, is run at the lowest priority, but on relatively fast PCs and assuming only a few real-time processes with no extreme rescheduling frequencies, there is no noticeable difference to the user.

The software environment consists of low level programs: *scope and dome drivers, cameraserver,*

HAT access module (HAM), and high level software: central database (DB) and virtual observer (“Observer”). See Fig. 4 for a schematic flowchart.

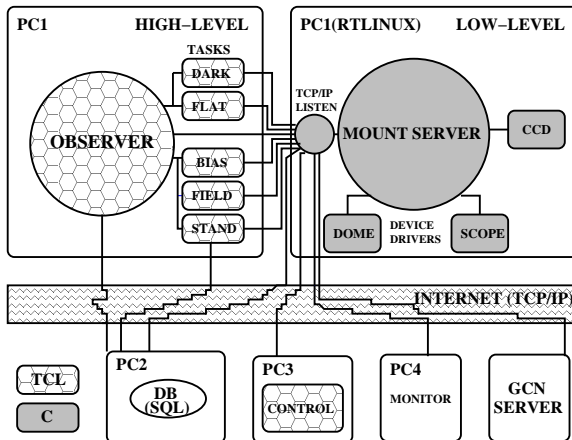


Fig. 4.— Overview of the software system: low and high level control, central database, remote control and monitoring via Internet. The “PC” inscriptions show a possible setup; the computers on which the given software run, although it is possible to run everything on a single PC. The programming language is indicated by the backgrounds.

3.1. Low level programs

The telescope mount’s kernel driver is mainly responsible for positioning the mount. It is a character device driver, i.e., complex commands can be issued to it as ascii strings, which are executed after being parsed. Status information is readable from a special file, showing relative positions in steps, RA and Dec, and so on. Both axes can independently track (with any sidereal rate), fine-slew or slew (maximal speed).

As mentioned in §2.1, acceleration and deceleration of the axes is done in finite angular-velocity, or in other words frequency steps, so as to minimize slip of the friction drive. The “infinite” accelerations between the finite velocity levels are in fact smoothed to continuity by the elasticity of the components. The driver also reads interrupts coming from the proximity sensors indicating the home or end positions. It can “home” the mount (move marked points on the horseshoe and declination discs precisely above the proximity sensors) from any unknown position, which is handy

⁷www.fsmlabs.com

for resetting the continuously accumulating slips, and for orientation if the telescope is “lost”. The home position’s hour angle and declination is calibrated at the installation of the telescope. After nulling values at the home position, the number of steps taken in any axis and any direction is always stored, and the residuals after a subsequent homing indicate the amount of slip. The tracking speed can be fine-tuned with a precision of 10^{-7} , which means that the hardware element’s absolute dimensions (e.g., the ratio of the driving roller to the diameter of the horseshoe) are not that restricted (but only important in absolute pointing). Finally, RA and Dec values can be assigned to any position.

The dome driver is a similar RTLinux kernel driver responsible for i) turning the main power on/off, ii) closing or opening the dome, iii) activating lens heating, iv) control of domeflat lights, v) detection of rain. Status of the dome can be queried from the driver.

CCD acquisition software of the Apogee AP10 CCD is based on the application programming interface from Pojmański (2002), modified to fulfill our needs. The camera server can run as a standalone application, or as a “daemon”, accepting commands from other software via Internet Protocol (TCP/IP).

The so-called HAT Access Module (HAM) is the main low-level program joining all the aforementioned codes. It accepts input via TCP/IP from higher level software (e.g., the virtual Observer), parses the commands, and distributes them to the relevant resources. That is, all telescope, dome and CCD operations are piped through this program. Another aspect of HAM is allocation of the drivers, i.e. no other program can issue conflicting commands to the hardware.

3.2. High level programs

We use the fast, reliable and open source relational Structured Query Language (MySQL⁸) database for storing associated parameters of the station (setup of mount, telescope, CCD, scheduled tasks, etc.), and for keeping continuously accumulating logs of operations (parameters of archived images, etc.), all of them arranged into

⁸Information on MySQL is available at www.mysql.org

tables. This has several advantages over simply keeping information in files without a database wrapper: i) faster operation on data, ii) TCP/IP access (for instance through the Internet), iii) use of existing interfaces to MySQL from various programming languages. The smooth TCP/IP communication enables installation of multiple HAT observatories in any preferred topology, with central database management, and with the possibility that the sites interact with each other, for example, request the last object observed or instruct another telescope.

The observatory as a whole is managed by the *virtual* Observer, which communicates with the access module, central database and executes (observer) programs. This is a Tcl⁹ language-based simulation of near-perfect observer, modeled as a finite-state machine, which makes decisions/transitions depending on the circumstances.

The Observer programs (such as taking flatfield frames and all-sky monitoring) are run as independent threads, so the Observer never hangs by waiting for a time-consuming operation to finish; it can be aborted any time. Tasks have start times (relative to sunset), allowed durations and priorities – both taken from the DB, whose properties are used by a task-manager (part of the Observer) to launch or stop them and to suspend or interrupt other tasks. There is a template, which makes writing new tasks very simple for the user, using a command library of a few hundred commands, such as “ObserveObject”.

During normal operation, the Observer is in “run” state. If the weather is unfavorable, the Observer passes to a “weather sleep” state, where the CCD is kept cooled, the dome is closed, and the system waits for clearing. In the daytime the system is in “daysleep”, power is turned off, CCD is warmed back, and we are waiting for the first scheduled task to appear within the characteristic time needed for starting up. If the Internet connection with the monitoring stations is lost, system jumps to “suspend” state, turns off power, and waits a long time before finally exiting to “service” state. Recovery from service is possible only by manually restarting the system.

Upon entering the “run” state, Observer checks the tasks to be executed during the given session,

⁹Information on Tcl is available at www.scripts.com

checks weather information, and if needed, starts up the system (turns power on, starts cooling the CCD). Following this, it enters an endless cycle, and breaks out only in case of transition to another state. During the cycle it responds to direct TCP/IP messages from outside, and checks if connection with the access module and outside-connection monitor is alive. The ephemerides are continuously updated, such as apparent position of the Sun and Moon. The task manager launches, checks or stops tasks, administrates changes in the DB. If a task exits abnormally, perhaps due to some kind of exception (programming error), it is flagged, and not launched again any more. Proper scheduling of tasks is one of most complex part in the code.

The weather status is checked every ~ 10 sec, and if needed, the current task is aborted, and the observatory transits to another state. There is a possibility of looking for targets of opportunity by parsing remote TCP/IP packets, such as the GRB Coordinates Network (GCN)¹⁰. The Observer checks and can take action upon incoming email communication, which enables the scientist to control or monitor the observatory even from a cellphone.

Eventually, with a given time resolution (~ 30 min), ConCam¹¹ (Pereira et al. 2000) all-sky night-time images and infrared satellite images¹² are downloaded and stored. These proved to be very useful later in flagging the photometric quality of a night. The Observer also has the ability to recover from various emergency situations (e.g., disk is full, device missing), and notify recipients via email.

Automatic start up of HAT is included in the booting procedure of the computer, similarly, closing the observatory in the shutdown phase. This way the service staff can easily start up/bring down the system. Also, HAT operations resume as the power outage ends.

4. Pointing precision of HAT

While highly accurate pointing of a telescope covering a 9 degree field might appear to be merely

a luxury, we tried to have a general purpose design with the flexibility of upgrading the focal length, thus decreasing the field of view, which requires more precise pointing. Moreover, sufficient pointing capability of even a wide field instrument can be relevant to its photometric precision. There are indications that precise aperture photometry depends on positioning the same star over the same pixels of the CCD, due to inter and intra-pixel variability (Buffington, Booth, & Hudson 1991; Robinson et al. 1995), although minute displacements of the telescope also do have advantages in filtering out internal reflections due to the fast focal ratio of the instrument. Due to our open-loop system, deviation of absolute pointing accumulates proportionally to the individual pointing accuracy, which has to be minimized.

Astrometric calibration was carried out at Konkoly Observatory, Budapest during the summer of 2001. We used a replica (HAT-2) of the mount at Kitt Peak, the Meade Pictor 416xt CCD, and a Soviet “MTO” 100mm \emptyset , f/10 Maksutov telephoto lens¹³. The 1m focal length and the fine, 1.86"/pixel resolution were useful for calibration, which used the starry sky as reference grid. Whenever needed, we made approximate correction for atmospheric refraction, and used Guide Star Catalogue (GSC; Lasker et al. 1990) for finding the astrometric solution of the frames, and coordinates of the central pixel.

We distinguish between the following attributes of pointing: *homing*, *tracking*, *absolute-pointing* precisions and *pointing repeatability*. In general, depending on the kind of precision, crucial factors can be the balance of the axes, ramping-up distance, maximal slewing speed, surface conditions and shape of the horseshoe, polar setting and orthogonality of the axes (RA, Dec, optical axis).

Homing precision measures how precisely can we set the mount to the home-position defined by the proximity sensors. The scatter of individual homings turned out to be $\sigma_{RA} = 0.5$ sec, $\sigma_{Dec} = 25''$.

The tracking of the system depends on adjustment of the polar axis, tracking speed (set by the mount driver), and the effect of environmental changes (e.g., strong wind) on the axes. The projected position of the mount’s polar axis on the

¹⁰<http://gcn.gsfc.nasa.gov/>

¹¹For more information: www.concam.net

¹²National Weather Service – www.wrh.noaa.gov

¹³Special thanks to A. Holl for lending us the lens.

sky was determined from the arcs of stars from exposures with $\approx 20\times$ sidereal tracking around the pole, during which the diurnal motion of the stars was negligible. As actual position of the celestial pole is known from astrometry databases, we could adjust the polar axis with $\pm 20\text{pix} \approx 0.5'$ precision.

The tracking was measured in calm weather conditions on fields culminating near zenith, from hour angle $HA \approx -1\text{h}$ to $HA \approx 1\text{h}$. Tracking speed was adjusted and then kept fixed in such a way that tracking residuals were minimal. The overall tracking error during 2 hours was less than 0.5sec in RA. We also found quasi-periodic errors with $\sim 20\text{min}$ characteristic timescale and 0.5sec amplitude, which were probably due to irregularities on the small RA roller (see Fig. 5).

We defined absolute pointing precision as the precision of moving the telescope to a celestial object (grid star) with respect to the home position or another star (reference star). Pointing errors scaled with the arc of movement, but overall scatter *without* removing any systematic error with a correction map were in the order of $\sigma_{\text{RA}} \approx 20\text{sec}$, $\sigma_{\text{Dec}} \approx 70''$. Repeatability was measured by moving the telescope back to the reference point, usually a bright star close to zenith. Repeatability is better than absolute pointing: $\sigma_{\text{RA}} \approx 7\text{sec}$, $\sigma_{\text{Dec}} \approx 50''$. This indicates that our absolute pointing errors – at least partly – originate from non-perpendicularity of the axes and imperfect polar axis setting.

5. Installation of HAT-1 on Kitt Peak

HAT-1 was transported (airmail) within its dome from Budapest to Steward Observatory, Tucson in January, 2001. The telescope was badly damaged during the trip, but thanks to Steward Observatory's hospitality, it was repaired in a few weeks. The telescope was installed to Steward Observatory, Kitt Peak in the following month, and was ready for operations by March 2001.

Our PC is hosted by the SuperLotis building's warmroom, and cables go out to the $\sim 2\text{m}$ high, massive concrete pillar on the western edge of the ridge, holding the HAT dome and telescope. The bug (§2.4) with the AP10 CCD delayed operation of HAT until mid-May, but finally Apogee serviced the camera.

The first few month period was devoted to de-

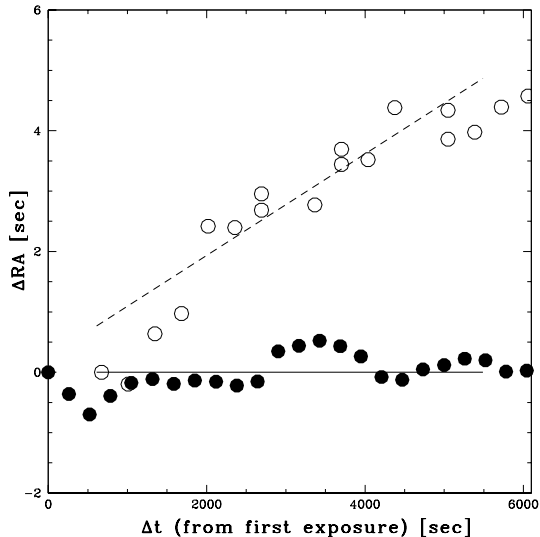


Fig. 5.— Tracking errors of HAT and MTO 100mm \varnothing lens in a 2 hour run. The upper line and empty circles show improperly tuned tracking speed. The lower line represents calibrated tracking. Deviations with characteristic time $\sim 10^3\text{sec}$ arise from the irregularities on the RA roller.

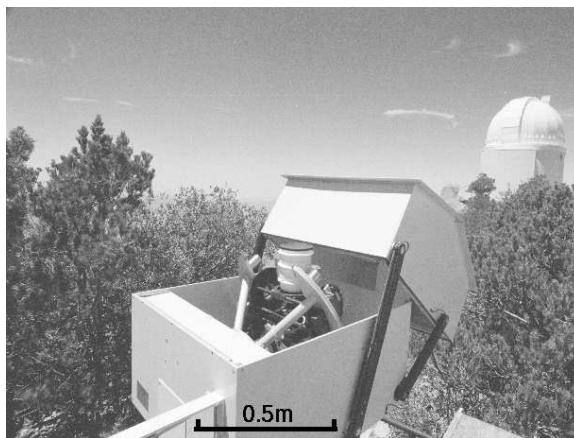


Fig. 6.— HAT-1 at Kitt Peak: asymmetric clamshell dome and horseshoe-mount. The white tube is the light baffle on the Nikon lens.

bugging the system and finalizing observing programs. Although HAT worked in robotic mode, its operation was monitored from Hungary. As reliable dome status (open/close) information is not available for any of the domes at Kitt Peak, we had to set aside the idea of slaving our dome opening to that of a manually operated telescope, and open/close jointly with the other dome. Thus, weather status was assessed at early Kitt Peak evening (5am Central European Time) from the Internet using the daytime webcam of Kitt Peak¹⁴, the National Weather Service forecast¹⁵ and ConCam images during the night. Some information is automatically downloaded and parsed by HAT, e.g. we switch to “weather-sleep” state if the wind sensors of the 4m Mayall telescope show gusts in excess of 45km/h.

During the debugging period we started regular observations of selected fields. The logfiles were examined next day, and updated software was transferred to the site by the next evening. This way, in a few months, the software became very reliable, and no major modifications have been performed since.

Since September, 2001, HAT has been operated from the Harvard-Smithsonian Center for Astrophysics, Cambridge, MA.

6. Observations from Kitt Peak

A typical observing session of HAT is described in the following. Roughly 1.5 hours before sunset, camera cooling is started, and after the service temperature is reached, 20 bias frames are taken. Following this, twenty 4-minute dark frames are exposed. If weather is clear, the “skyflat” task starts up 10 minutes after sunset. After opening the dome, HAT selects an optimal flatfield region from the database, which is close to the preferred point of minimal sky gradient (Chromey & Haselbacher 1996). This point is usually opposite to the Sun in azimuth, and 20° from zenith. The telescope is randomly moved between skyflat frames so as to permit median averaging out brighter stars, and exposure time is recursively tuned to keep the central intensity at $\sim 50\%$ of saturation. Even with these considerations, the twilight sky on

a $9^\circ \times 9^\circ$ area has gradients up to 10%, and therefore we installed a domeflat screen. Unfortunately this brought up further complications, and domeflat observations are still under development. At the end of the night session, skyflats, darks and biases are taken again.

The monitoring of selected fields (“monfield”) starts when the Sun sinks 11° below the horizon. The entire sky was split up into 696 slightly overlapping fields, each $8^\circ \times 8^\circ$ wide. Choosing the next field to be observed is done by a sophisticated algorithm. A list of enabled fields is loaded from the database, and visible ones with high enough elevation are selected. Visibility means that the object is within the limits of the mount, above the artificial horizon-grid, and far enough from the Sun and Moon ($\gtrsim 45^\circ$). Ranking of the fields is done by combining their previous observation times (the more recent, the lower rank), their proximity to the meridian or the western horizon (depending on the ranking method) and manually set priorities from the database. After any observation, parameters (e.g. time of last observation) are updated and synchronized with the DB. This ensures that none of the regions are observed too frequently until there are other, favorably situated fields. Fields close to culmination, thus having the smallest possible airmass and differential refraction, are not missed. Priorities of fields can be such that given their visibility, they are observed with higher frequency, or even exclusively. Finally, a small random factor is appended to the ranks in order to avoid the same selection on two consecutive nights, thus daily aliases in frequency analysis. The telescope is homed every hour to keep pointing accuracy.

Our present observing tactic is to observe most of the visible fields sparsely, for information on long-time variation, and only concentrate on a few fields for short-term variability. The high priority is re-assigned to different fields on a weekly - monthly timescale. With two consecutive, randomly displaced 240s exposures per field, we can carry out photometry in the range of $I_c \approx 6 - 13^m$. We also experimented with 30s exposures so as not to lose information on very bright, saturated stars, but this increased the data flow without considerable amount of extra photometric information. With this approach we collect about 80 (winter) to 50 (summer) frame-pairs per clear night, which

¹⁴<http://www.noao.edu/cgi-bin/kpno/axim.cgi>

¹⁵<http://www.wrh.noaa.gov>

means approx. 30 photometric points per night and star for high priority fields (10^6 photometric measurement altogether).

Calibration of the data to standard I_c -band is not straightforward, as we currently observe only with a single I_c filter. Either Hipparcos Catalogue stars (van Leeuwen et al. 1997) in our fields are used for direct calibration, or we observe Landolt standards (Landolt 1983, 1992) throughout the night. In both cases we have to restrict ourselves to color-independent terms:

$$i_{inst} = I_c + \xi_i + k_i \cdot X - \dot{\xi} \cdot (t - t_0),$$

where i_{inst} and I_c are the instrumental and (close to) standard magnitudes, X is the airmass, t is the time from an arbitrary epoch t_0 , and ξ_i , k_i , $\dot{\xi}$ are coefficients to be determined by the regression.

Observation of Landolt standards is performed by the “standard” task, which selects suitable standard stars (bright enough, not extreme colors, have large airmass and hour-angle span), and observes the star with fine time and airmass resolution plus the culminating fields. This task is launched maximum few times a month, during absolute-photometric, new-moon nights.

Current data flow with lossless compression is $\sim 1.6\text{Gb/day}$ (winter) to 1Gb/day (summer), thus new DAT DDS-3 tapes have to be inserted every week.

The only unautomated procedures in HAT operation are checking weather status at evening (rain is detected automatically, but clouds not) and tape changing.

During a year’s operation HAT has completed approx. 140 observing sessions, with a total number of ~ 35000 exposures of which 19000 were field observations, the rest were calibration frames.

7. Photometric precision of HAT

Reduction of the current 160Gb of data is under way. Photometric precision of HAT-1 at Kitt Peak was tested using a 12-night subset of images from September/October 2001 for the moderately crowded field “F077” ($\alpha = 23^{\text{h}}15^{\text{m}}00^{\text{s}}, \delta = 48^{\circ}00'00''$). This contains only about 5% of our current data set. We primarily concentrate on the repeatability of the measurements, i.e., the precision for generating light-curves (in a system as

close to I_c as possible) as compared to the *accuracy*, which is relative to absolute standards. Our crude estimate for the latter from Hipparcos I-band stars, standard star observations and the problematic flatfielding is that absolute calibration errors can be as high 0.1^{m} in the field corners, but less than 0.05^{m} in the center.

A summary of the sessions is listed in Table 1. Observations were taken during a servicing mission, thus calibration frames are not available for all nights, and the system was not providing its maximal performance. Baffle on the lens was installed only in January 2002, and overscan region of the chip was not read out properly. The field was observed to zenith angles as high as 60° .

Table 1: Summary of HAT-1 test observations

Date	N	Bias	Dark	Flat	Moon	Com
21/09	43	0	0	0	20%	Clear
22/09	62	0	0	0	30%	Clear
24/09	42	0	0	0	50%	Clear
25/09	52	0	14	53	60%	Clear
26/09	38	16	18	0	70%	Clear
27/09	32	4	18	0	80%	
04/10	58	20	18	0	99%	
05/10	62	26	18	34	90%	Cirrus
10/10	36	25	18	35	50%	Cirrus
12/10	26	19	18	3	20%	Cirrus
13/10	26	24	18	34	15%	Cirrus
14/10	27	24	18	29	10%	Cirrus

NOTE.— The table only shows data used for finding out the photometric precision of HAT-1, and comprises $\sim 5\%$ of the complete data set. “Date” format is day/month, year 2001. “N” denotes the number of frames for field F077. “Moon” is the phase of the Moon.

Calibration of frames was done in a standard way, and consisted of bias and dark subtraction, and flatfield correction. Time-dependence of bias level was not dealt with. For some of the nights dark frames were not available, however the dark pattern seems to change in time. Calibration was done by our Tcl interface to IRAF ¹⁶ (Tody 1993).

As mentioned in §6, flatfielding with skyflat

¹⁶IRAF is distributed by the National Optical Astronomy Observatories, which are operated by the Association of Universities for Research in Astronomy, Inc., under cooperative agreement with the National Science Foundation.

frames of a 9° wide field is problematic. We tried to remove the large scale pattern (partly due to division with flatfields not truly representing the response function of the system) by blank-sky correction, using median average of frames taken at moonless, clear nights, close to zenith, and far from the Milky Way. Unfortunately even these frames should be treated with caution because in some cases gradients from zodiacal light or the rippled structure of the night airglow were easily visible, and confirmed from ConCam images.

Astrometry of the master frame was performed by IRAF/GEOMAP, GEOXYTRAN, and the residuals (offsets in arcseconds) of the second order polynomial transformation between the celestial reference frame and the image were in the order of $\sigma \approx 0.8''$.

Photometry of images was finally done by the aperture photometry routine in the IRAF/DAOPHOT package (Stetson 1987) after experimenting with ISIS-2.1 Image Subtraction Method (Alard 2000) without positive results due to our undersampling (fwhm=1.6 – 2.0 pixel). The bottleneck in the latter method seemed to be spatial interpolation of the images to the reference grid, and re-sampling the narrow psfs. Experiments with IRAF/GEOTRAN to get around this problem did not significantly improve the results.

An astrometric reference image was montaged from 20 individual frames by transforming them to the same reference grid. A starlist was established by DAOFIND (60K stars), and later the same IDs were assigned to the same stars on all frames for easy cross-identification. This astrometric reference was useful *only* for finding sources with good efficiency, but due to the resampling of narrow psfs during the transformation of individual images, it was not used in photometry at all.

We found roughly 30K stars per individual frame down to a threshold of 5 sigma of the background with DAOFIND. Background scatter ($\sigma_{\text{bg}} \approx 10 - 20\text{ADU}$) almost entirely comes from the sky (mean level $\approx 300\text{ADU}$ at new moon) and processing noise (Newberry 1991), while readout noise ($R \approx 2\text{ADU}$), digitization noise ($T \approx 0.29\text{ADU}$), etc., are negligible. The raw photometric data was first transformed to the master frame in the XY-plane, stars were cross-identified, IDs were re-assigned.

A reference magnitude file was created by averaging individual raw photometry measurements for a dozen good quality images. Magnitudes for all frames were shifted to this reference, where the amount of the shift was spatially dependent, typically done on a 6×4 XY-grid, and few hundred stars for each block. The residuals of the transformation indicated our photometric precision, and were in the order of $\sigma \approx 0.01^{\text{m}}$. Spatial dependence is a reasonable assumption due to the wide field-of-view and differential extinction. Some fraction of the scatter is due to color-dependence of extinction, which we cannot take into account. Standard calibration of the field was tied to non-saturated Hipparcos stars.

After construction of the light-curves, we could estimate the photometric precision of the system by assuming that most of the stars are constant, and by deriving the rms of the light-curves around their mean values. Most light-curves have 250 data points, and each point is the result of $2 \times 240\text{s}$ exposures. Comparison with the formal error of individual points given by the photometry code (based upon the flux of the star, the background, and various parameters) showed that the formal error underestimates our rms with stars brighter than $I \sim 10^{\text{m}}$, while slightly overestimates at faint sources (see Fig. 7). We also derived the J_s Stetson variability index for each star (Stetson 1996) following Kaluzny et al. (1998), where the formal errors are scaled by a linear relation to the true errors (Fig. 7, lower panel).

Stars with at least 100 data points and $J_s > 0.75$ were selected as suspected variables (~ 1700). After standard Fourier analysis, the selection was further narrowed by looking only at periods shorter than 25^{d} and Signal Detection Efficiency (Alcock et al. 2000; Kovács et al. 2002) of the main peak in the power spectrum greater than 4.5. Finally, 60, mostly short period light-curves were selected by hand (see Fig. 8). We cross-correlated the list with the General Catalogue of Variable Stars (Kholopov et al. 1998, GCVS), including the New Suspected Variables (NSV), and found only 12 known and 1 suspected variables. Stars were also looked up in the Hipparcos (Perryman et al. 1997b), Tycho-2 (Høg et al. 2000) catalogues, Tycho variable stars (Piquard et al. 2001), and

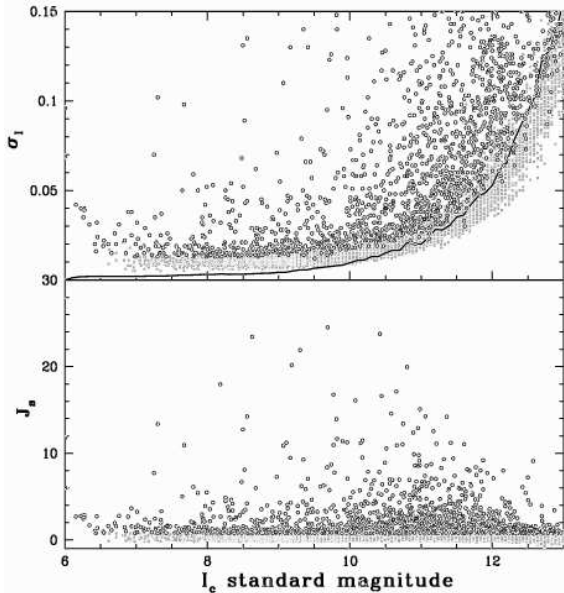


Fig. 7.— Photometric precision of HAT with 8 minute exposures. The upper panel shows the rms of light-curves, which contain at least 100 points. Open circles denote stars with J_s variability index greater than 0.75, i.e., suspected variables, while gray points mark constant stars. The solid line shows the average *estimated* error by DAOPHOT. The lower panel shows the variability index for the same stars.

the Simbad database¹⁷, but only one (out of those not in the GCVS) was found with variability flag (GSC 0362701580 in Fig.8). Eight stars out of the suspected new discoveries were in the well-known BD, HD or SAO catalogues.

In addition, we retrieved all variables in our FOV from the GCVS catalogue having brighter maximum than 13^m , not being saturated on our images, and having a period shorter than 25^d (14 entries). Ten out of them were found by our survey, one was too crowded, and omitted from the original coordinate lists (CZ And), another variable was too elongated in the corner of our field, thus not found by DAOFIND. CU And, semi-detached binary was excluded from our selection due to its small variability index ($J_s = 0.5$), although it has a good quality light-curve. Finally,

¹⁷We acknowledge the use of the SIMBAD database, operated at CDS, Strasbourg, France: simbad.u-strasbg.fr

FL Lac was faint and crowded, and our light-curve was too noisy for selection.

The 46 new variables are marked with their GSC numbers. Several long-period variables were also found, but due to the limited time-span of our observations, we do not include them in the present paper.

8. Summary and future directions

We described a small, autonomous observatory, which has been working for one year at Steward Observatory, Kitt Peak. In spite of the small telephoto lens used as the “telescope”, it can perform massive photometry of bright sources. It completed on the order of 20000 pointings to different objects, yielding a data flow of $\sim 10^6$ photometric measurements per night, and proved to work reliably. Using 5% of our data, and a single selected field, a few dozen bright ($I < 13$) variables were found, further reinforcing the incompleteness even on the bright end of previous variability searches. Some parameters of the system are summarized in Table 2.

HAT-1 is capable of monitoring a *small fraction* of the sky with sufficient time resolution. Multiple filters would not only ease classification of sources based upon their colors, but due to differential refraction (vs. color), the photometric precision would be also improved. Wider aperture would increase the incoming flux, and either our time-resolution at constant photometric precision would drop, or our limiting magnitude with the same exposure times would be expanded. This would not be necessarily *improvement* of the system, but in some sense the target of observations would be different. HAT is designed to operate in a network. It is an off-the-shelf system of $\sim 15K$ USD cost, plus the CCD. These make multiple installations easy. It is also a flexible, multi-purpose observatory, not only eligible for all-sky monitoring, but could be used as a photometric monitor station at bigger observatories. Current bottleneck is neither hardware development or operating HAT, but rather efficient data reduction, archiving and web-availability of the data. After efficient software can handle the data flow and overcome the difficulties, we plan to upgrade HAT with more filters, bigger telescopes, and to install multiple stations.

Table 2: Specification of HAT-1 at Kitt Peak.

Equatorial mount	
Max. RA slew	2°/sec
Max. Dec slew	5°/sec
RA resolution	1"/step
Dec resolution	5"/step
Max. tel. diam.	20cm
CCD (Apogee AP10)	
Dimensions	2K × 2K, 14 micron
Gain	10 e-/ADU
Readout noise	2 ADU
Dark current	0.05ADU/sec at -15°C
Readout time	< 10s
Cooling	Peltier ($\Delta T = 32^\circ C$)
Lens (Nikon 180mm f/2.8)	
Aperture	65mm
Plate scale	16"/pixel
Field of view	9° × 9°
Pointing precision	
Homing	< 0.5'
Tracking	< 0.5sec/2hr
Absolute	RA:20sec, Dec: 1'
Repeatability	RA: 7sec, Dec: 1'
Photometry (I_c band, 8min time res.)	
Accuracy (absolute)	$\approx 0.05^m$
Precision ($I_c < 10^m$)	$\lesssim 0.01^m$
$I_c = 11^m$	0.02 ^m
$I_c = 12^m$	0.05 ^m

9. Acknowledgements

This project was initiated by Prof. Bohdan Paczyński. We are grateful for his tireless support, encouragement, advice and funds from the generous gift of Mr. William Golden. We are indebted to G. Pojmański for his collaboration and for sharing his plans and software with us. It is a pleasure to thank P. Strittmatter the opportunity of installing HAT to Kitt Peak, the partial funds in the installation costs and the hospitality of Steward Observatory. We are thankful to the whole staff of Steward Observatory (B. Peterson, G. Stafford, W. Wood, J. Rill) for their consistent support in operating HAT. G. Bakos wishes to acknowledge the kind hospitality of Konkoly Observatory during the test period of HAT, while being an undergraduate and junior research fellow, with special thanks to the director, L. G. Balázs.

The project was partially funded by the Hungarian OTKA T-038437 grant. Support is also acknowledged to NASA grant NAG 5-10854. G. Bakos is greatly indebted to the Smithsonian Astrophysical Observatory for support through the SAO Predoctoral Fellowship program. We thank G. Kovács, R. W. Noyes, D. D. Sasselov, K. Z Stanek and A. H. Szentgyorgy for valuable discussions and their careful reading of this manuscript.

REFERENCES

- Alard, C. 2000, *A&AS*, 144, 363.
- Alcock, C. et al. 2000, *ApJ*, 542, 257.
- Allsman, R. A. & Axelrod, T. S. 2001, *astro-ph/0108444*
- Akerlof, C. et al. 2000, *AJ*, 119, 1901.
- Antipin, S. 1997, *A&A*, 326, L1.
- Bakos, G. Á. 2001, *RTLinux driven HAT for All Sky Monitoring*, *Smale Telescope Astronomy on Global scales*, Eds. B. Paczyński, Claudia Lemme, Wen Ping Chen, *ASP Conf. Series*, 246, 59 (IAU coll. 183)
- Borucki, W. J., Caldwell, D., Koch, D. G., Webster, L. D., Jenkins, J. M., Ninkov, Z., & Showen, R. 2001, *PASP*, 113, 439.
- Boyd, L. J., Genet, R. M., Sauer, D. J., Hawthorn, P. S., Slonaker, L. W., & Chatto, J. 1984, *BAAS*, 16, 909.
- Brown, T. M. & Charbonneau, D. 1999, *American Astronomical Society Meeting*, 195, 110907.
- Buchler, J. R., Serre, T., & Kolláth, Z. 1995, *Physical Review Letters*, 73, .
- Buffington, A., Booth, C. H., & Hudson, H. S. 1991, *PASP*, 103, 685.
- Burki, G., Schmidt, E. G., Arellano Ferro, A., Fernie, J. D., Sasselov, D., Simon, N. R., Percy, J. R., & Szabados, L. 1986, *A&A*, 168, 139
- Chen, W. P. 1999, *Observational Astrophysics in Asia and its Future*, 181.
- Chromey, F. R. & Hasselbacher, D. A. 1996, *PASP*, 108, 944.

- Duerbeck, H. W. et al. 2000, *AJ*, 119, 2360.
- Helmer, L. & Morrison, L. V. 1985, *Vistas in Astronomy*, 28, 505.
- Høg, E. et al. 2000, *A&A*, 357, 367.
- Ishioaka, R. et al. 2001, *IAU Circ.*, 7669, 1.
- Kaluzny, J., Stanek, K. Z., Krockenberger, M., Sasselov, D. D., Tonry, J. L., & Mateo, M. 1998, *AJ*, 115, 1016.
- Kholopov, P. N. et al. 1998, *Combined General Catalogue of Variable Stars (GCVS)*, (VizieR Online Data at CDS, Strasbourg: II/214A)
- Kiss, L. L., Szatmáry, K., Szabó, G., & Mattei, J. A. 2000, *A&AS*, 145, 283.
- Kovács, G., Zucker, S. & Mazeh, T. 2002, *A&A*, accepted
- Landolt, A. U. 1983, *AJ*, 88, 853.
- Landolt, A. U. 1992, *AJ*, 104, 340.
- Lasker, B. M., Sturch, C. R., McLean, B. J., Russell, J. L., Jenkner, H., & Shara, M. M. 1990, *AJ*, 99, 2019.
- van Leeuwen, F., Evans, D. W., Grenon, M., Grossmann, V., Mignard, F., & Perryman, M. A. C. 1997, *A&A*, 323, L61.
- Leung, K. 1962, *JRASC*, 56, 242.
- Macri, L. M., Sasselov, D. D., & Stanek, K. Z. 2001, *ApJ*, 550, L159.
- Nakano, S. & Kushida, Y. 1996, *IAU Circ.*, 6323, 1.
- Newberry, M. V. 1991, *PASP*, 103, 122.
- Paczynski, B. 1997, *Variables Stars and the Astrophysical Returns of the Microlensing Surveys*, Edited by R. Ferlet, J. P. Maillard and B. Raban, 357.
- Paczynski, B. 2000, *PASP*, 112, 1281.
- Park, H. S. et al. 1997, *ApJ*, 490, L21.
- Park, H. S. et al. 2001, *American Astronomical Society Meeting*, 198, 3805.
- Pereira, W. E., Nemiroff, R. J., Rafert, J. B., Ftacelas, C., & Perez-Ramirez, D. 2000, *American Astronomical Society Meeting*, 197, #115.10.
- Perryman, M. A. C. et al. 1997, *The HIPPARCOS and TYCHO Catalogues*, ESA SP-1200, Vol. 1-17
- Perryman, M. A. C. et al. 1997, *The HIPPARCOS and TYCHO Catalogues*, ESA SP-1200, 1, 465, http://astro.estec.esa.nl/Hipparcos/vis_stat.html
- Piquard, S., Halbwegs, J.-L., Fabricius, C., Geckeler, R., Soubiran, C., & Wicenec, A. 2001, *A&A*, 373, 576, also *VizieR Online Data Catalog* 337, 330576
- Pojmański, G. 1997, *Acta Astronomica*, 47, 467.
- Pojmański, G. 1998, *Acta Astronomica*, 48, 35.
- Pojmański, G. 2000, *Acta Astronomica*, 50, 177.
- Pojmański, G. 2002, private communication
- Smith, D. A. et al. 2002, *astro-ph/0204404*
- Richmond, M., Treffers, R. R., & Filippenko, A. V. 1993, *PASP*, 105, 1164.
- Robinson, L. B., Wei, M. Z., Borucki, W. J., Dunham, E. W., Ford, C. H., & Granados, A. F. 1995, *PASP*, 107, 1094.
- Stetson, P. B. 1987, *PASP*, 99, 191.
- Stetson, P. B. 1996, *PASP*, 108, 851.
- Tody, D. 1993, *ASP Conf. Ser. 52: Astronomical Data Analysis Software and Systems II*, 2, 173.
- Walker, A. 1987, *Noao Newsletter No. 10*, 16
- Woźniak, P. R. et al. 2002, *astro-ph/0201377*

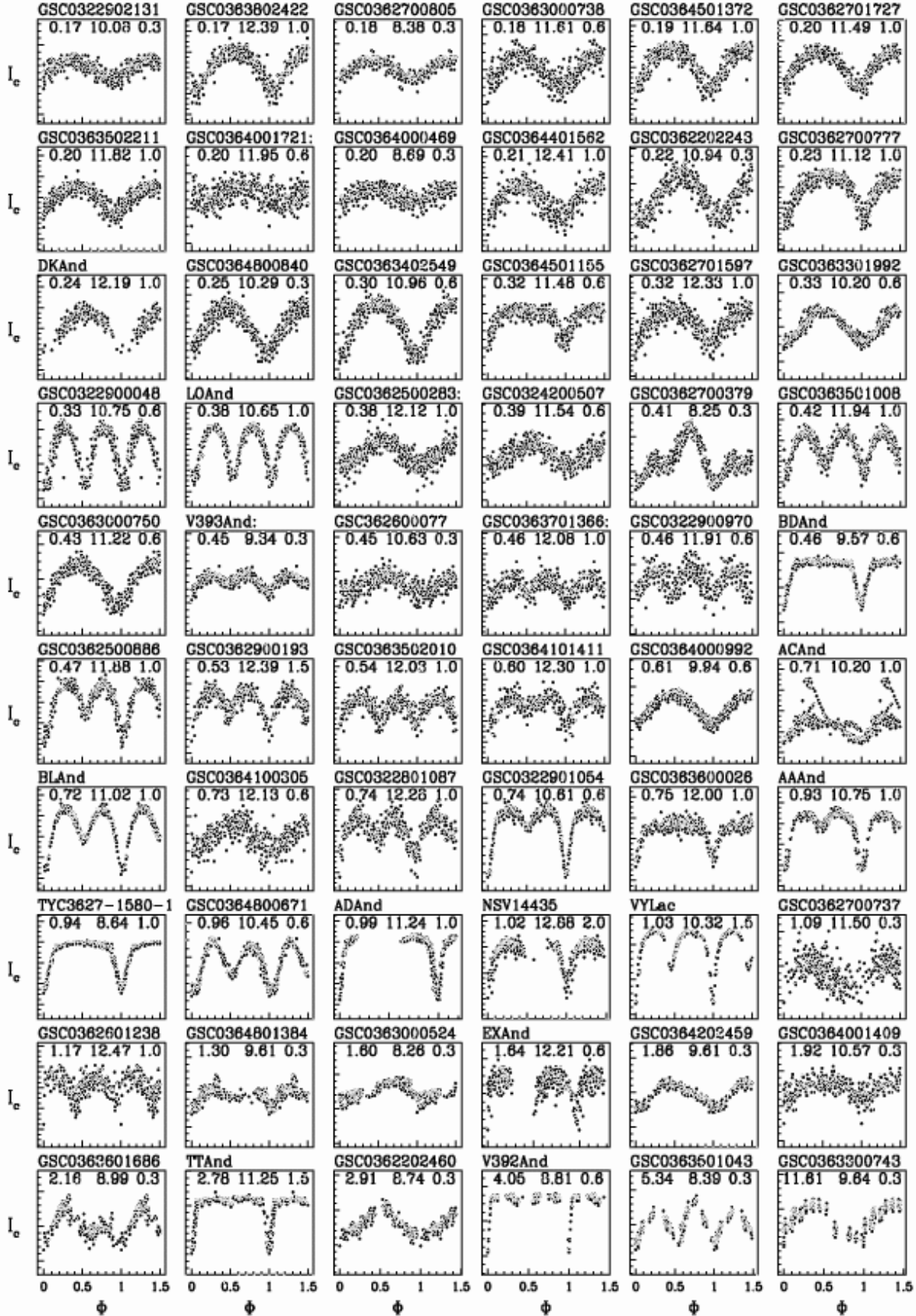


Fig. 8.— Selected variables from HAT observations of field “F077”. Known variable stars are marked with their conventional names, new discoveries with their GSC numbers. Numbers in the panels indicate the period, average I-band brightness and the height of the box (magni-